ChemPubSoc Europe

DOI: 10.1002/cphc.201301051

The Effect of Cholesterol on Membrane Dynamics on Different Timescales in Lipid Bilayers from Fast Field-Cycling NMR Relaxometry Studies of Unilamellar Vesicles

Carla C. Fraenza,[a] Carla J. Meledandri,[b, c] Esteban Anoardo,*[a] and Dermot F. Brougham*[b]

The general applicability of fast field-cycling nuclear magnetic resonance relaxometry in the study of dynamics in lipid bilayers is demonstrated through analysis of binary unilamellar liposomes composed of 1,2-dioleoyl-*sn*-glycero-3-posphocholine (DOPC) and cholesterol. We extend an evidence-based method to simulating the NMR relaxation response, previously validated for single-component membranes, to evaluate the effect of the sterol molecule on local ordering and dynamics over multiple timescales. The relaxometric results are found to be most consistent with the partitioning of the lipid molecules into affected and unaffected portions, rather than a single averaged phase. Our analysis suggests that up to 25 mol%, each cholesterol molecule orders three DOPC molecules, providing experimental backup to the findings of many molecular dynamics studies. A methodology is established for studying dynamics on multiple timescales in unilamellar membranes of more complex compositions.

1. Introduction

Understanding the dynamics and phase behavior of binary lipid membranes is a key challenge in biophysical science. In the first instance, these model systems provide a proving ground for developing experimental methods and theoretical formalisms that can be subsequently applied to ternary systems, and perhaps ultimately to biological membranes. Secondly, while the coexistence of stable liquid phases is probably thermodynamically unfavorable in binary systems, the presence of submicron regions, or domains, containing altered properties is generally accepted.[1] New insights into the dynamics, composition and lifetimes of domains in binary membranes are a step towards a more complete picture of the assembly and dissolution of domains in membranes in general. In particular, the effect of cholesterol on membrane dynamics has been intensively studied. Numerous works applying a wide range of experimental techniques have shown that the sterol molecule affects the lateral ordering of the lipids in the liquid disordered (l_d) phase, while at higher concentrations and lower temperatures phase separation into liquid-disordered and liquid-ordered phase (l_o) has been described.[2,3,4]

Most of the experimental methods that have been applied to elucidate membrane dynamics are sensitive to a particular dynamic timescale. For instance fluorescence techniques, such as fluorescence recovery after photo-bleaching (FRAP), have been applied to many membrane compositions and structures including both giant and small unilamellar vesicles. A wealth of information on lipid diffusion (a dynamic process on an intermediate timescale) and on acyl chain ordering has been obtained.[5,6] The dynamics of the spy fluorophore within the lipid mixture (usually phosphatidylcholine/cholesterol) is a complicating factor for interpretation, as the composition is no longer strictly binary.[7] Nuclear magnetic resonance (NMR) techniques have also been prominently applied and they are sensitive to a range of timescales: NMR lineshape analysis is sensitive to the 10^{-4} to 10^{-6} s timescale. Pulsed field gradient PFG-NMR techniques can also be used to study lateral diffusion, $\sim 10^{-5}$ s, but usually only for macroscopically oriented lipid bilayer stacks,[2,8] or multi-lamellar vesicles.[9,10]

Fast field-cycling NMR relaxometry (FFC NMR) has the distinct advantage that it is sensitive to motions over a comparatively wide timescale, from 10^{-3} to 10^{-9} s, and it can be used to study hydrated sub-micron sized liposomes in suspension. In FFC NMR the spin-lattice relaxation rate (R_1) is recorded as a function of magnetic field strength ($\mathbf{B}_0$), and hence ^{1}H Larmor frequency, as $\nu_0 = \gamma^H \mathbf{B}_0/2\pi$, where γ^H is the ^{1}H gyromagnetic ratio. Spectroscopic information cannot be obtained due to inhomogeneity of the rapidly switchable $\mathbf{B}_0$ field. However, detailed dynamic information is obtained from the macroscopic evolution of the net ^{1}H magnetization, which is determined by the time dependence of the nuclear spin interactions, as modulated by a range of dynamic processes. FFC NMR is sensi-

[a] C. C. Fraenza, Prof. E. Anoardo
Laboratorio de Relaxometría y Técnicas Especiales
Grupo de Resonancia Magnética Nuclear
Facultad de Matemática, Astronomía y Física
Universidad Nacional de Córdoba and IFEG (CONICET)
Córdoba (Argentina)
E-mail: anoardo@famaf.unc.edu.ar

[b] Dr. C. J. Meledandri, Dr. D. F. Brougham
National Institute for Cellular Biotechnology
School of Chemical Sciences
Dublin City University, Dublin 9 (Ireland)
E-mail: dermot.brougham@dcu.ie

[c] Dr. C. J. Meledandri
Department of Chemistry and
MacDiarmid Institute for Advanced Materials and Nanotechnology
University of Otago, Dunedin (New Zealand)

tive to dynamic processes over a wide range of timescales and has been successfully applied to study dynamics in an extensive range of materials.[11]

We have previously described a model for interpreting the FFC NMR ^{1}H spin-lattice relaxation rate dispersions (NMRD profiles) of single component unilamellar liposomes, LUVs, in the l_d phase.[12] LUVs are a better model system as unlike multi-lamellar vesicles, MLVs,[13] they produce a stable NMR response over the timescale of the experiment, this aspect is discussed fully in our original study.[12] The model was successfully validated for liposomes prepared with different lipids (DMPC and DOPC), sizes (100–200 nm) and temperatures, using values for the different physical constants and parameters available in the literature.[14] Hence the approach was shown to be a useful tool for the study of the dynamic and viscoelastic properties of single component membranes. Within our model the relaxation rate, R_1, can be described by Equation (1):

$$R_1 = \frac{1}{T_1} = A_{OF}J_{OF}(\omega) + A_D J_D(\omega) + A_R J_R(\omega) + A_{FM}J_{FM} \quad (1)$$

where T_1 is the spin-lattice relaxation time, $J_{OF}(\omega)$, $J_D(\omega)$ and $J_R(\omega)$ are the spectral densities corresponding to order fluctuations (due to shape fluctuations of the liposome sphere), translational and rotational diffusion, respectively. A_j are the corresponding amplitudes reflecting the strength of the relevant ^{1}H-^{1}H dipolar interactions. $\omega = 2\pi\nu_0$ and $A_{FM}J_{FM}$ is a constant to account for the faster motions, which are not dispersive within the frequency window explored.

The field dependence (0.03–11.7 T) of the ^{31}P and ^{13}C spin-lattice relaxation rates for a variety of phospholipid mixtures in small and large unilamellar vesicles has been successfully measured by other authors using high-resolution field-cycling ^{31}P[15,16] and ^{13}C[17] NMR. A significant difference between high-resolution ^{31}P and ^{13}C techniques and low-resolution field-cycling ^{1}H NMR relaxometry used in our work are the spin interactions that drive relaxation. An important contribution to the relaxation mechanism in the high-resolution case is the chemical shift anisotropy. In the region where dipolar interactions are dominant (below 1 T), only a few significant data points are available for ^{31}P (although more data was recorded for the ^{13}C case). The authors analysed the data using a model-free approach,[18,19] which is a clear contrast with our interpretation of the ^{1}H relaxometry in terms of well-established dynamic models, incorporating physical parameters from independent techniques. The high-resolution technique is very powerful for studying dynamics of individual molecular segments, which can be compared with simulations. However, critically the approach does not provide insights into the membrane collective dynamics.

In this paper we confront the issue of whether there are one or two lipid populations, in model binary membranes of phosphatidylcholine and cholesterol, with new experimental data as a further development of our established method. We analyze experimental NMRD profiles obtained at 298 K for liposomes of radius between 68 and 80 nm, composed of DOPC with cholesterol concentrations of 10 and 25 mol%, and obtain insights into membrane motions, over many orders of magnitude in time, that are consistent with independent physical measurements. The profiles are shown to be most consistent with the partitioning of the lipid molecules into affected and unaffected portions rather than a single averaged phase. We find that up to 25 mol% cholesterol, each sterol molecule orders three DOPC molecules, which is a rare experimental confirmation of the results of extensive simulation. The implications of these findings and the potential that is now evident for the approach to be applied to the study of curved membranes in general are discussed.

2. Results and Discussion

2.1. Results and Analysis

Experimental profiles were analyzed in two different ways. Firstly, the model was applied under the assumption that the membrane was in the disordered liquid crystalline phase (l_d), with its viscoelastic properties modulated according to the cholesterol content. Within this picture, we used data available in the literature that accounts for the influence of cholesterol on the average viscoelastic properties of the membrane (as they are reflected in the measured physical parameters). This treatment will be referred to as the single population approach.

Secondly, we considered two different kinds of lipid populations: those strongly affected by the presence of a nearby cholesterol molecule, and those lipids sufficiently far from a cholesterol molecule to be completely unaffected. We will refer to this procedure as the two-population approach. The boundary between these two populations/regions is defined by a cholesterol-induced radius of action (R_a) centred at every cholesterol molecule. A graphical representation of the lipid organization in this model is shown in Figure 1. As discussed below, our view is that the populations represent exchanging or fluctuating fractions.

The unaffected lipids were considered completely free of any cholesterol influence. That is, they were considered to be in the l_d phase having the same dynamics already described for single component liposomes. The affected lipids, whose local order is much increased due to the influence of the cholesterol, were considered for the purposes of calculation, to be in the l_o phase. This relaxometric description was implemented, within our established model, using physical parameters corresponding to this ordered phase. As a result, we have Equation (2) to simulate the experimental data:

$$\begin{aligned} R_1 = & R_1^{unaff} + R_1^{aff} = \frac{N^{unaff}}{N}\left[A_{OF}^{unaff}J_{OF}^{unaff}(\omega) + A_R^{unaff}J_D^{unaff}(\omega)\right] \\ & + \frac{N^{aff}}{N}\left[A_{OF}^{aff}J_{OF}^{aff}(\omega) + A_D^{aff}J_R^{aff}(\omega)\right] + A_{FM}J_{FM} \end{aligned} \quad (2)$$

where the superscripts unaff and aff refer to unaffected and affected lipids, respectively; N is the total number of DOPC lipids in the sample; N^{unaff} and N^{aff} represent the number of unaffected and affected lipids, respectively, as given by Equations (3)

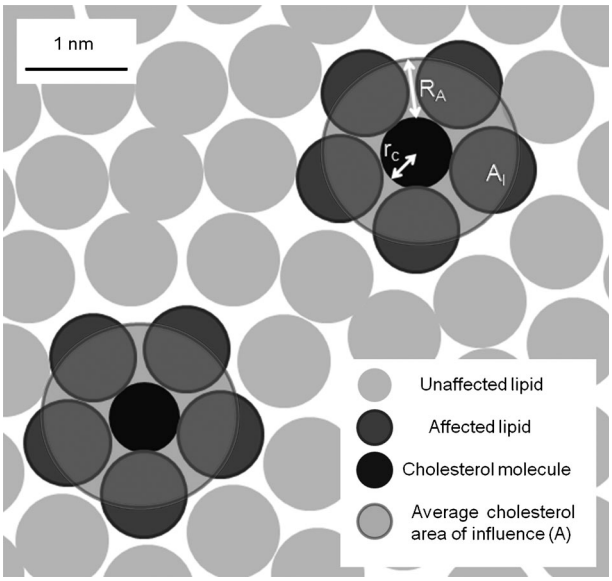

Figure 1. Graphical representation of the two population approach. The circles represent the lipids and cholesterol molecules. The viewpoint is from a position perpendicular to the plane of the bilayer.

and (4):

$$N^{unaff} = N - N^{aff} \quad (3)$$

$$N^{aff} = N_C(A/A_l) \quad (4)$$

Here N_C is the total number of cholesterol molecules in the sample; $A = [\pi(R_a + r_C)^2 - \pi.r_C^2]$ is the average cholesterol area of influence, r_C is the cholesterol average radius and R_a the average cholesterol radius of influence. A_l is the average area of the affected lipids (see Figure 1). $J_{OF}(\omega)$, $J_D(\omega)$, $J_R(\omega)$ are the spectral densities corresponding to order fluctuations, diffusion, and molecular rotational dynamical processes, respectively. The A_j values are the corresponding amplitude prefactors, defined as $(9/8r^6)\gamma^4\hbar^2(\mu/4\pi)^2$ where r_j is the effective ^1H–^1H distance for the relevant dynamic process.

Single-Population Approach

Profiles recorded at 298 K for DOPC LUVs and the simulated curves using the single-population approach with: a) 10 mol% cholesterol and average radius $R_0 = 80$ nm, and; b) 25 mol% cholesterol and an average radius of $R_0 = 68$ nm, are shown in Figures 2 and 3, respectively, with the corresponding model parameters given in the Tables 1 and 2. Errors were determined by analyzing the sensitivity of the simulated curve to variations of each parameter. The error interval given corresponds to the maximum shift of the simulation curve within experimental error (approximately the size of data points).

Using this approach it was possible to obtain simulated profiles consistent with the experimental data for both cholesterol percentages. The values for the physical quantities used are within the expected range according to literature (compare Tables 1 and 2 with Table 5). Note that the values for 0% cholesterol in Tables 1 and 2 are adjusted to take into account the difference in liposome size, using our established model for the size dependence of single-component membranes.[14]

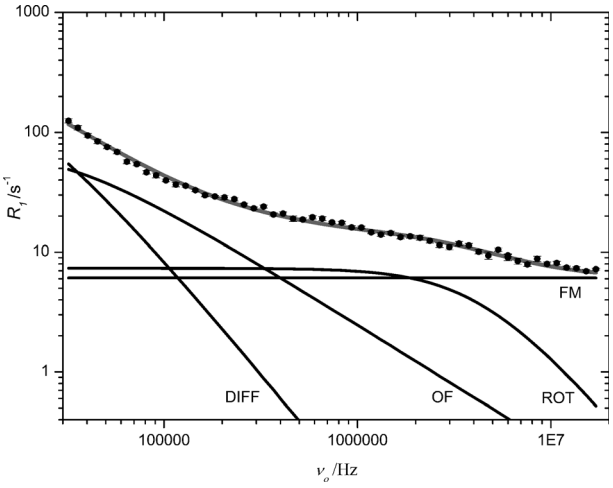

Figure 2. Experimental relaxation profile for DOPC + 10 mol% cholesterol liposomes with average radius $R_0 = 80$ nm, recorded at 298 K (●). The simulated curve using the single-population approach is shown in grey solid line. Contributions from each type of motion are included in black soild lines: order fluctuations (OF), diffusion (DIFF), rotation (ROT), and fast motions (FM). The relevant parameters are given in Table 1.

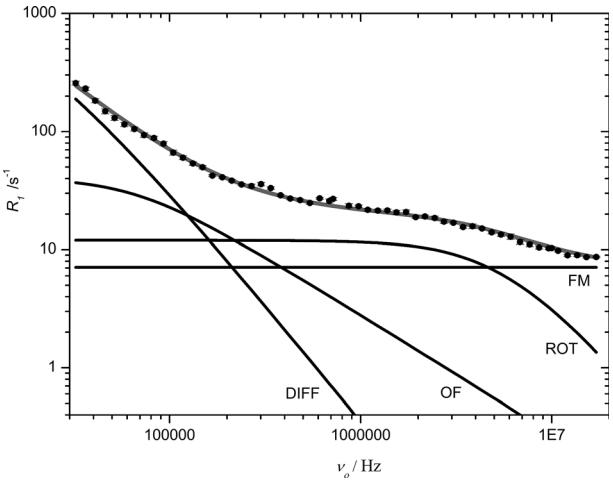

Figure 3. Experimental relaxation profile for DOPC + 25 mol% cholesterol liposomes with average radius $R_0 = 68$ nm, recorded at 298 K (●). The simulated curve using the single-population approach is shown in grey solid line. Contributions from each type of motion are included in black soild lines: order fluctuations (OF), diffusion (DIFF), rotation (ROT), and fast motions (FM). The relevant parameters are given in Table 2.

The trends in the key parameters, shown in both Tables 1 and 2, suggest changes in membrane properties associated with the inclusion of cholesterol in the membrane, broadly in line with expectation. The elastic modulus increases (stiffer membrane), the diffusion coefficient decreases and the lipid rotational correlation time increases. Our approach has previously been shown to reproduce the expected size and temperature dependencies of the key parameters for single-component membranes.[14] These results demonstrate that it can be extended to multi-component compositions, which is very encouraging.

Table 1. Parameters corresponding to the simulation of the relaxation profile using the single population approach, recorded at 298 K for DOPC LUVs with 10 mol% cholesterol and an average radius R0 = 80 nm. The parameters corresponding to free-cholesterol DOPC LUVs at the same temperature and average radius are shown for comparison (see Figure 2). The percentage change in the parameters is also included.

Parameter	Model value		Change %
Cholesterol %	0	10	–
η D_2O [K g s^{-1} m^{-1}]	1.1×10^{-3}	1.1×10^{-3}	–
σ	0	0	–
a [nm]	1	1	–
κ [J]	$(5.4\pm0.8)\times10^{-20}$	$(6.3\pm0.9)\times10^{-20}$	17
A_{OF} [s^{-2}]	$(1.0\pm0.3)\times10^{9}$	$(1.4\pm0.3)\times10^{9}$	40
D [m^{2}s^{-1}]	$(1.3\pm0.4)\times10^{-11}$	$(0.7\pm0.2)\times10^{-11}$	−46
τ_D [s]	$(0.7\pm0.2)\times10^{-4}$	$(1.2\pm0.3)\times10^{-4}$	71
A_D [s^{-2}]	$(1.0\pm0.3)\times10^{9}$	$(1.2\pm0.4)\times10^{9}$	20
τ_R [s]	$(1.1\pm0.3)\times10^{-8}$	$(2.1\pm0.5)\times10^{-8}$	91
A_R [s^{-2}]	$(1.0\pm0.3)\times10^{8}$	$(0.7\pm0.2)\times10^{8}$	−30
$A_{FM}J_{FM}$ [s^{-1}]	(5±1)	(6.1±0.9)	22

Table 2. Parameters corresponding to the simulation of relaxation profile using the single-population approach, recorded at 298 K for DOPC LUVs with 25 mol% cholesterol and an average radius R_0 = 68 nm. The parameters corresponding to free-cholesterol DOPC LUVs at the same temperature and average radius are shown for comparison (see Figure 3). The percentage change in the parameters is also included.

Parameter	Model value		Change %
Cholesterol %	0	25	–
η D_2O [K g s^{-1} m^{-1}]	1.1×10^{-3}	1.1×10^{-3}	–
σ	0	0	–
a [nm]	1	1	–
κ [J]	$(5.4\pm0.9)\times10^{-20}$	$(8\pm1)\times10^{-20}$	48
A_{OF} [s^{-2}]	$(1.0\pm0.3)\times10^{9}$	$(2.0\pm0.4)\times10^{9}$	100
D [m^{2}s^{-1}]	$(8.8\pm0.3)\times10^{-12}$	$(5.5\pm0.8)\times10^{-12}$	−38
τ_D [s]	$(0.7\pm0.2)\times10^{-4}$	$(1.0\pm0.1)\times10^{-4}$	43
A_D [s^{-2}]	$(1.3\pm0.2)\times10^{9}$	$(3.5\pm0.3)\times10^{9}$	170
τ_R [s]	$(1.1\pm0.3)\times10^{-8}$	$(1.6\pm0.3)\times10^{-8}$	45
A_R [s^{-2}]	$(2.0\pm0.3)\times10^{8}$	$(1.5\pm0.2)\times10^{8}$	−25
$A_{FM}J_{FM}$ [s^{-1}]	(5±1)	(7.1±0.8)	42

Two-Population Approach

Simulated curves were also generated for different relative quantities of affected and unaffected lipids [Eq. (2)] using the following procedure, which is designed to reduce the possibility of over-fitting. The parameters corresponding to the dynamics of the unaffected lipids were fixed. These are the same as for the 0% cholesterol case, adjusted for liposome size (as in the single-population approach). The parameters corresponding to dynamics of the affected lipids were fixed within their most probable intervals, according to the literature values for the l_o phase. One of ten values between 10% and 100% was selected for the fraction of affected lipids, by selecting the value for the cholesterol radius of action, R_a. The parameters for the affected lipids (l_o phase) were adjusted, within the most probable interval, for each R_a value to determine the optimal simulated curve. This was done manually by looking for the best agreement between the simulation and experimental data. From this curve we extract the most probable values for the ordered phase.

The optimal R_a value (the fraction of affected lipids) was determined by minimizing the sum of the squared differences (SSD) between the simulated and experimental values, defined by Equation (5):

$$\mathrm{SSD} = \sum_i \left(R_{1i}^{\mathrm{exp}} - R_{1i}^{\mathrm{sim}}\right)^2 \quad (5)$$

where R_{1i}^{exp} and R_{1i}^{sim} represent the experimental data and the corresponding simulated R_1 values at ν_{0i}, respectively. The smaller the SSD, the more accurately the simulation reproduces experiment, see Figures 4 and 5.

With this procedure we are able to determine the cholesterol radius of action, that is, the average number of affected lipids, N^{aff}, for each cholesterol concentration. As formulated in Equation (2), the N^{aff} value is assumed to be the same for all the dynamic modes. However, the number of affected lipids could be sensitive to the timescale of the different modes. Clearly, our model provides an estimate of N^{aff}. That is the number we obtain is a spatially and temporally averaged value determined directly from the dynamics of all the motions that drive fluctuations in the ^{1}H–^{1}H dipolar interactions of the total lipid. It can be compared to the numbers of ordered lipids obtained from molecular dynamics simulation. However, N^{aff} has the advantage that it is derived, subject to an acceptable model for the contributing dynamic processes, from experiment. In that way N^{aff} differs from almost all other determinations of the affected fraction, this point is discussed further below.

We applied this treatment to the interpretation of the profiles of DOPC LUV suspensions recorded at 298 K with:

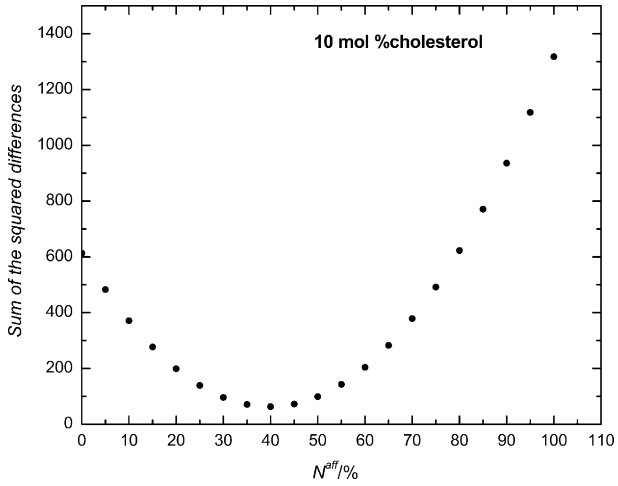

Figure 4. Sum of the squared differences of simulated and experimental profiles using the two-population approach as a function of percentage of affected lipids for DOPC + 10 mol% cholesterol liposomes, average radius R_0 = 80 nm, at 298 K. The minimum shows that the optimal simulated dispersion curve corresponds to 40% of affected lipids.

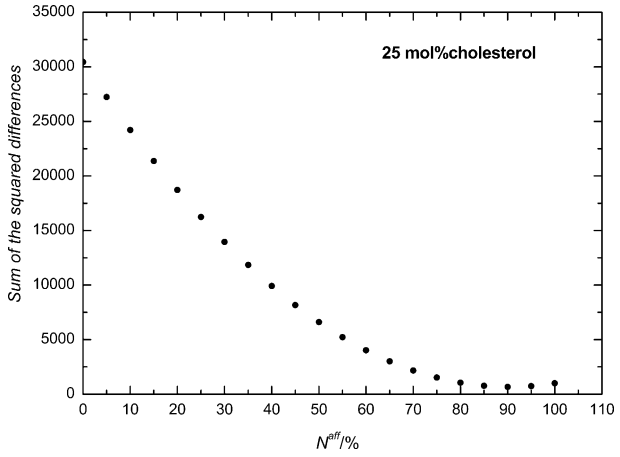

Figure 5. Sum of the squared differences of simulated and experimental profiles using the two-population approach as a function of percentage of affected lipids for DOPC + 25 mol% cholesterol liposomes, average radius $R_0 = 68$ nm, at 298 K. The minimum shows that the optimal simulated dispersion curve corresponds to 90% of affected lipids.

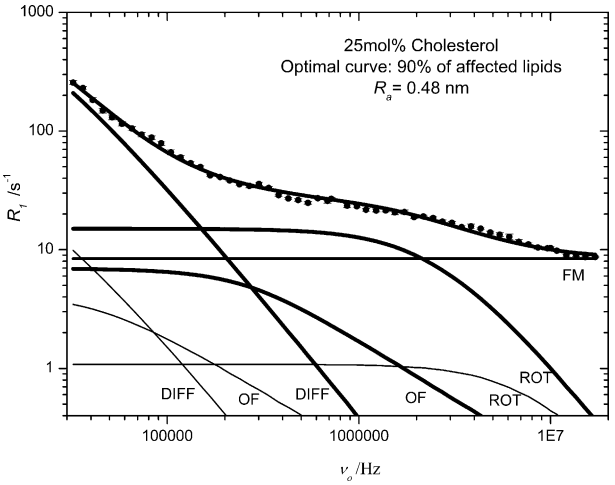

Figure 7. Experimental relaxation profile for DOPC + 25 mol% cholesterol liposomes, average radius $R_0 = 68$ nm, recorded at 298 K (●). The optimal simulated dispersion curve using the two-population approach corresponds to 90% of affected lipids (grey solid line). Contributions from each type of motion are included in black soild lines for affected (thicker lines) and unaffected lipids: order fluctuations (OF), diffusion (DIFF), rotation (ROT), and fast motions (FM). The relevant parameters are included in Table 4.

a) 10 mol% cholesterol and average radius of $R_0 = 80$ nm, and b) 25 mol% cholesterol with an average radius of $R_0 = 68$ nm. In Figures 4 and 5, the SSD values are shown as a function of the percentage of affected lipids for both cholesterol compositions. Minima appear at 40% and 90% of affected lipids, for 10 and 25 mol% cholesterol, respectively. The experimental and simulated profiles corresponding to these N^{aff} values are presented in Figures 6 and 7, and the corresponding parameters are given in Tables 3 and 4, again for 10 and 25 mol% cholesterol, respectively.

The results obtained clearly show that it is also possible to generate simulated profiles that are in very good agreement with experimental data for both cholesterol concentrations using the two-population approach. The numerical values used for the optimal simulations are in the expected literature range (compare Table 3 and Table 4 with Table 5). The analysis produces optimal N^{aff} values of 40% affected lipids ($R_a = 0.63$ nm) for 10 mol% cholesterol, and 90% ($R_a = 0.48$ nm) for 25 mol% cholesterol. The average number of affected lipids for each cholesterol molecule is ~3. Note that the values of and the changes in the key parameters (Tables 3 and 4) are consistent with physical expectation. However, the appearance of the spectral density contributions from the two populations, shown in Figures 6 and 7, largely reflect the key parameter, N^{aff}.

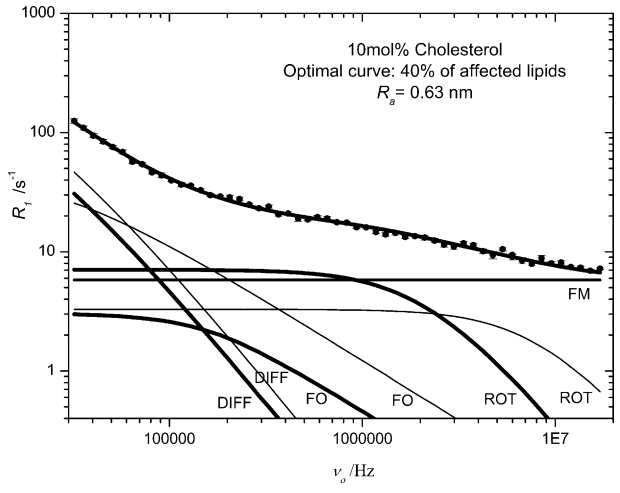

Figure 6. Experimental relaxation profile for DOPC + 10 mol% cholesterol liposomes, average radius $R_0 = 80$ nm, recorded at 298 K (●). The optimal simulated dispersion curve using the two-population approach corresponds to 40% of affected lipids (grey solid line). Contributions from each type of motion are included in black solid lines for affected (thicker lines) and unaffected lipids: order fluctuations (OF), diffusion (DIFF), rotation (ROT), and fast motions (FM). The relevant parameters are included in Table 3.

2.2. Discussion

Studies of Cholesterol in Model Membranes

The effect of cholesterol on membrane dynamics has been intensively studied and numerous works have shown that the molecule strongly affects the lateral organization of the other lipids. The general view is that at a microscopic level cholesterol causes an increase in the order parameters of acyl hydrocarbon chains by reducing the number of trans-gauche isomerizations. This is supported by spectroscopic[57,58] and other evidence, and it is found that the effect is stronger for saturated hydrocarbon chains.[59] However, rapid lipid rotation and lateral diffusion continue to occur in the fluid phase.[60] At lower cholesterol concentrations and higher temperatures membranes in the liquid disordered phase (l_d) retain liquid-like properties, while at higher concentrations and lower temperatures phase separation into liquid-disordered and liquid-ordered phase (l_o) has been described,[3,4] largely based on the superposition of characteristic ^{2}H NMR patterns.

For binary mixtures of cholesterol with low T_m lipids, such as 1,2-dioleoyl-*sn*-glycero-3-posphocholine (DOPC), PFG-NMR

Table 3. Parameters for the simulation of the relaxation profile using the two-population approach with 40% of affected lipids. Corresponds to data recorded at 298 K for DOPC LUVs with 10 mol% cholesterol and an average radius $R_0 = 80$ nm (see Figure 6).

Parameter	Model value	
	Unaffected lipids (l_d phase)	Affected lipids (l_o phase)
η D_2O [$Kg\,s^{-1}\,m^{-1}$]	1.1×10^{-3}	1.1×10^{-3}
σ	0	0
a [nm]	1	1
Cholesterol area [nm^2]	–	0.35
Lipid area [nm^2]	0.73	0.71
K [J]	$(5.4\pm0.8)\times10^{-20}$	$(30\pm10)\times10^{-20}$
A_{OF} [s^{-2}]	$(1.0\pm0.3)\times10^{9}$	$(3\pm2)\times10^{9}$
D [m^2s^{-1}]	$(1.3\pm0.4)\times10^{-11}$	$(0.5\pm0.2)\times10^{-11}$
τ_D [s]	$(0.7\pm0.2)\times10^{-4}$	$(1.5\pm0.5)\times10^{-4}$
A_D [s^{-2}]	$(1.0\pm0.3)\times10^{9}$	$(2.1\pm0.9)\times10^{9}$
τ_R [s]	$(1.1\pm0.3)\times10^{-8}$	$(4.4\pm0.9)\times10^{-8}$
A_R [s^{-2}]	$(1.0\pm0.3)\times10^{8}$	$(0.8\pm0.1)\times10^{8}$
$A_{FM}J_{FM}$ [s^{-1}]	(5.8 ± 0.6)	
R_a [nm]	–	0.63
Number of lipids affected by cholesterol	–	3.6

Table 4. Parameters for the simulation of the relaxation profile using the two-population approach with 90% of affected lipids. Corresponds to data recorded at 298 K for DOPC LUVs with 25 mol% cholesterol and an average radius $R_0 = 68$ nm (see Figure 7).

Parameter	Model value	
	Unaffected lipids (l_d phase)	Affected lipids (l_o phase)
η D_2O [$Kg\,s^{-1}\,m^{-1}$]	1.1×10^{-3}	1.1×10^{-3}
σ	0	0
a [nm]	1	1
Cholesterol area [nm^2]	–	0.35
Lipid area [nm^2]	0.73	0.64
K [J]	$(5.4\pm0.9)\times10^{-20}$	$(30\pm10)\times10^{-20}$
A_{OF} [s^{-2}]	$(1\pm0.3)\times10^{9}$	$(5.1\pm1.9)\times10^{9}$
D [m^2s^{-1}]	$(8.8\pm0.3)\times10^{-12}$	$(5.5\pm0.8)\times10^{-12}$
τ_D [s]	$(0.7\pm0.2)\times10^{-4}$	$(1.0\pm0.1)\times10^{-4}$
A_D [s^{-2}]	$(1.3\pm0.2)\times10^{9}$	$(4.3\pm0.4)\times10^{9}$
τ_R [s]	$(1.1\pm0.3)\times10^{-8}$	$(3.7\pm0.5)\times10^{-8}$
A_R [s^{-2}]	$(2.0\pm0.3)\times10^{8}$	$(0.9\pm0.1)\times10^{8}$
$A_{FM}J_{FM}$ [s^{-1}]	(8.4 ± 0.2)	
R_a [nm]	–	0.48
Number of lipids affected by cholesterol	–	2.7

measurements have shown that, at compositions where there may be multiple domains, there is rapid molecular exchange between the pools, which must therefore be sub-micron in scale.[2,47] It was also suggested that the system remains in the l_d phase up to 40 mol%, at room temperature. Indeed it is generally accepted that for binary compositions, sub-micron domains are better described as fluctuations rather than persistent, or stable, thermodynamic phases.[1] The lateral diffusion of different sterols and POPC or DPPC in mixed membranes was also investigated by pulsed field gradient magic angle spinning ^{1}H NMR spectroscopy (PFG MAS ^{1}H NMR).[9,10] The method combines the high resolution of MAS with the ability to measure apparent diffusion coefficients for all resolved components in the mixture, for example, lateral diffusion of the sterol and phospholipid in the same membrane, without the use of perturbing labels. The findings were in broad agreement with the PFG-NMR studies on oriented layers.[2,47] It was shown that the boundaries between liquid-ordered and liquid-disordered domains are not insurmountable

Table 5. Summary of the most probable intervals for each physical parameter in the l_d phase and l_o phase with indicative references.

Parameter	l_d phase range			Refs.	l_o phase range	Refs.
Cholesterol molar percent	0[a]	10[b]	25[c]	–	≥ 35 ≤ 50[d]	–
η D_2O [$Kg\,s^{-1}\,m^{-1}$]	$(0.8–1.3)\times10^{-3}$	$(0.8–1.3)\times10^{-3}$	$(0.8–1.3)\times10^{-3}$	[20, 21]	$(0.8–1.3)\times10^{-3}$	[12, 13]
σ	0–25	0–25	0–25	[20, 22, 23]	0–25	[12, 14, 15]
a [nm]	1–1.2	1–1.2	1–1.2	[24–27]	1–1.2	[16–19]
Cholesterol area [nm^2]	–	0.32–0.39	0.32–0.39	[28–31]	0.32–0.39	[20–23]
Lipid area [nm^2]	0.71–0.74	0.7–0.72	0.64–0.69	[31–34]	–	–
k [J]	0.4×10^{-20}–1×10^{-19}	$(6.1–8.8)\times10^{-20}$	$(6.4–8)\times10^{-20}$	[32, 33, 35–37]	$3.5k_{ld} \leq k_{lo} \leq 6k_{ld}$	[30, 31]
A_{OF} [s^{-2}]	1.6×10^{7}–9.9×10^{9}	1.6×10^{7}–9.9×10^{9}	1.6×10^{7}–9.9×10^{9}	[40, 41]	1.6×10^{7}–9.9×10^{9}	[32, 33]
D [m^2s^{-1}]	10^{-12}–10^{-10}	$(5.8–7)\times10^{-12}$	$(4.9–6)\times10^{-12}$	[2, 8, 21, 26, 42–46]	$D_{ld}/4 \leq D_{lo} \leq D_{ld}/2$	[2, 5, 39–41]
A_D [s^{-2}]	1.6×10^{7}–9.9×10^{9}	1.6×10^{7}–9.9×10^{9}	1.6×10^{7}–9.9×10^{9}	[40, 41]	1.6×10^{7}–9.9×10^{9}	[32, 33]
τ_R [s]	10^{-10}–10^{-7}	10^{-10}–10^{-7}	10^{-10}–10^{-7}	[13, 50, 51]	$2\tau_R^{ld} \leq \tau_R^{lo} \leq 4\tau_R^{ld}$	[41]
A_R [s^{-2}]	1.6×10^{7}–9.9×10^{9}	1.6×10^{7}–9.9×10^{9}	1.6×10^{7}–9.9×10^{9}	[40, 41]	1.6×10^{7}–9.9×10^{9}	[32, 33]
R_a [nm]	–	0.5–3	0.5–3	[28, 29, 52–55]	0.5–3	[20, 21, 45–48]
Number of lipids affected by cholesterol	–	1–9	1–9	[52, 53, 56]	1–9	[45, 46, 49]

[a] Compare to Tables 1–4. [b] Compare to Table 1. [c] Compare to Table 2. [d] Compare to Tables 3 and 4.

for diffusion of phospholipid and sterol. The sterol diffusion rates were also found to depend on the sterol affinity to the phospholipids, with cholesterol showing the strongest interactions/slowest diffusion. However, it is difficult to translate these results directly to our study as multi-lamellar liposomes were used, which as noted above, are not stable under our conditions. The lateral diffusion may also differ for fully hydrated single bilayers. Significant decreases in diffusion on addition of cholesterol were also noted from EPR studies,[61] although once again these were typically performed on MLVs. In addition molecular spin labels (effectively additional components) are required, so the composition is not strictly binary.

Turning to the high-resolution field-cycling studies, the ^{1}H–^{31}P dipolar contribution to the ^{31}P relaxation was approximated by a field-dependent term, corresponding to a single correlation time τ_c, which was assumed to be the dominant low-field contribution. This dynamic process, which is on the 10^{-8} s timescale, was initially attributed to rotations of the whole lipid molecule around its long axis and/or torsional motions of the phosphate group,[15] and subsequently to a wobble in the cone describing the vectors connecting the ^{31}P nucleus to the two nearest glycerol ^{1}H.[16] The addition of cholesterol dramatically affects the low-field relaxation dispersion, increasing the τ_c value. While consistent with our findings for molecular rotations, the author's interpretation does not allow direct assessment into the potential influence of collective dynamics on the ^{1}H-induced ^{31}P relaxation. Comparison of the ^{13}C and with the ^{31}P case,[17] showed that the correlation time for the motion is the same for both cases in the presence of cholesterol. However, in the cholesterol free sample, the correlation time obtained from ^{31}P data is shorter, probably due to a faster local motion that becomes dampened in the presence of the sterol. The dynamic wobble process is apparently present with and without cholesterol. As such a motion cannot be uncorrelated in the presence of other lipids forming the membrane, one could speculate that it is the connection between the local and collective dynamics (it corresponds to the hydrodynamic mode whose damping time can be associated with the extracted τ_c value). Unfortunately, the quality of the data currently attainable with the high-resolution experiment, and the lack of spectral resolution in FFC NMR preclude a definitive study at this time.

On the other hand, molecular dynamics (MD) simulations have been very widely applied to study the energy landscape of lipid molecules (usually phosphatidylcholines) in bilayers in the vicinity of cholesterol and they provide an alternative picture. These studies suggest that, contrary to the description used in most experimental studies (fluorescence and PFG-NMR), the lipid pool is partitioned into fractions of affected and unaffected lipids depending on their proximity to a cholesterol molecule.[28,29,52,53,55] The former are commonly considered to be in the l_o phase and the latter in l_d. The consensus that emerges from the molecular dynamics simulations is that at moderate content the cholesterol molecules are dispersed across each layer[55] and each one orders a small number of lipid molecules[53] usually within the first neighbors (R_a ca.1 nm), although some authors have claimed a more longer range, but gradually weakening effect.[55]

MD simulations have potential to provide an atomic-scale picture of structural and dynamical properties of lipid membranes that complements and assists in the interpretation of experimental results. Among the effects of cholesterol studied by simulation[62,63] are the condensing effect, that is, the tendency of cholesterol to reduce the area or volume per lipid in bilayers, the increase of bilayer thickness and in the hydrocarbon chain (deuterium) order parameter, the decrease of cholesterol average tilt angle, and a weakening of water bridges between lipid molecules. It has also been shown[62] that cholesterol has a significant influence on the lipid dynamical processes on the sub-nanosecond time scale, including; headgroup flip-flop, chain defect motion along the acyl chains, partial rotation of the molecule as a whole, and single-molecule protrusion and lateral rattling-in-a-cage motions. It is likely that these motions are important for the lateral and trans-bilayer transport of small molecules. Therefore, the increase of the microscopic viscosity of the bilayer interior with cholesterol content, obtained identified from simulations is consistent with the observed reduction in passive bilayer permeability. MD simulations have also been used to study the hydrogen-bonding network within binary membranes.[64] It was concluded that each cholesterol molecule is hydrogen-bonded to no more than two lipids, with the interaction with saturated being favored over unsaturated lipids.

In the approach of Miao and Mouritsen[65] Monte Carlo importance sampling was used to obtain a statistical ensemble of microscopic states according to the Boltzmann distribution. The model incorporates a large number of sterols and PCs evolving under an approximate interaction potential with translational and molecular conformational degrees of freedom, and with a minimal model of the interactions between the molecules. From the simulation data the equilibrium conformational order parameter is obtained. Thread-like micro-domains were identified as a key feature. Cholesterol was found to have increased capacity, as compared to lanosterol, to stabilize the l_o phase.

Despite the obvious strength of computational methods they remain somewhat limited even today. In the case of MD the number of molecules included (100 s of lipid molecules) remains quite low, and in particular the total time of the MD simulations (100s of ns range) remains short. New insights into the dynamics, composition and lifetimes of domains in binary membranes from experimental studies are required to develop this picture. We believe that the approach described here has potential to contribute to that effort.

Fast Field-Cycling Relaxometric Study of Binary Membranes

Firstly, our results and analysis strongly suggest that the model previously used to explain the relaxation profile in single-component liposomes[12,14] can be extended to the study of binary liposomes containing cholesterol in the membrane. However, as two models can be used to reproduce the experimental

profiles a full evaluation of their relative merits is required. We shall look first at the statistical quality of the simulations.

Considering the single-population approach, the value of SSD for the simulation with 10 mol% was about 4.4 times smaller than that for 25 mol% cholesterol. On the other hand for the two-population approach, the SSD value for 10 mol% was about 10 times smaller than for 25 mol% cholesterol. Clearly both approaches provide a better reproduction of the experimental profile at lower cholesterol content. This probably arises because the cholesterol dynamics, which become more important at higher content, are not included independently. The SSD values also provide a means to compare the single- and two-population approaches. In the case of 10 mol% cholesterol, the SSD of the single population was about 3.3 times larger than for the two-population approach. On the other hand, in the case of 25 mol% cholesterol, the corresponding factor was about 1.4. The SSD values suggest that the two-population approach provides a better description of the experimental data. Although the interpretation of the key N^{aff} values, used in this model, requires some independent validation. Comparisons between the results obtained for the two cholesterol molar percentages using the two approaches are provided in Table 6.

In the case of the single-population approach it was assumed that cholesterol induces a modulation of the viscoelastic parameters of the entire membrane that remains in the disordered liquid crystalline phase, l_d, at 298 K. The results are consistent, for both compositions, with the observations of other authors that can be found in the literature.[2,47] The obtained parameters are within the expected range (according to the literature) for both cholesterol percentages (compare Tables 1 and 2 with Table 5). Comparing the values of τ_D for 0, 10 and 25 mol% cholesterol, the expected slight increase with cholesterol content can be noted.[2,45,46] A similar behaviour can be observed for the values of τ_R.[39] These results suggest that the cholesterol slows down the translational and rotational diffusion processes. The bending elastic modulus k shows a slight increase with the cholesterol content, also in agreement with other studies reported in the literature.[33,37] This result was attributed to a more rigid and ordered structure of the lipids in the presence of cholesterol.[28–30,37,48,52,59,66–74] All of these effects confirm that the essential aspects of the physical changes induced by cholesterol are captured by the FFC NMR approach, one of its main advantages is that it provides all of the information, for processes occurring over a very different timescales, from a single experiment.

The amplitude pre-factors did not show a very large change with the addition of cholesterol, but their variations were bigger for the case of 25 mol% cholesterol (see Tables 1 and 2). We attribute this effect to dynamics of the cholesterol molecule; as the concentration increases, cholesterol molecules contribute to the ^{1}H signal and their own dynamics start to be relevant. Since we did not include a special term reflecting the cholesterol dynamics, this contribution becomes absorbed into the lipid pre-factors. This approximation is equivalent to the implicit assumption that the cholesterol dynamics follows or mirrors the lipid dynamics, which in principle is reasonable for diffusion, in agreement with other authors,[9] and order fluctuations. This interpretation is also supported by the fact that the simulation using the single-population approach is closer to the experimental profile for the 10% cholesterol case, as noted above. The model could be further refined to account for cholesterol dynamics. However, a more physically intuitive improvement of the model is to partition the total lipid.

The two-population approach was inspired by results from computational simulations, mostly involving molecular dynamics,[28,29,52,53,55] which partition the lipid population into those in a region around each cholesterol molecule which are strongly ordered, and non-affected disordered lipids outside these regions. The simulated ^{1}H relaxation profiles obtained by splitting the population agree very well with experimental data for both cholesterol compositions.

The key step in applying this methodology was identifying the optimal R_a, by statistical comparison of experiment and simulation. The results suggest that there are about 3 affected lipids for each cholesterol molecule. This finding is consistent

Table 6. Comparative analysis of the most important physical parameters for the simulation of the relaxation profiles, recorded for DOPC LUVs with 10 and 25 mol% cholesterol at 298 K, using the single- and the two-population approaches.

Parameter	Single-population approach (l_d phase)	Two-population approach 60% unaffected lipids (l_d phase)	40% affected lipids (l_o phase) $R_a = 0.63$ nm	Single-population approach (l_d phase)	Two-population approach 10% unaffected lipids (l_d phase)	90% affected lipids (l_o phase) $R_a = 0.48$ nm
Cholesterol molar percent	10	0	10	25	0	25
R_o [nm]	80	80	80	68	68	68
κ [J]	$(6.3\pm0.9)\times10^{-20}$	$(5.4\pm0.8)\times10^{-20}$	$(30\pm10)\times10^{-20}$	$(8\pm1)\times10^{-20}$	$(5.4\pm0.9)\times10^{-20}$	$(30\pm10)\times10^{-20}$
A_{OF} [s^{-2}]	$(1.4\pm0.3)\times10^{9}$	$(1.0\pm0.3)\times10^{9}$	$(3\pm2)\times10^{9}$	$(2.0\pm0.4)\times10^{9}$	$(1.0\pm0.3)\times10^{9}$	$(5.1\pm1.9)\times10^{9}$
D [m^2s^{-1}]	$(0.7\pm0.2)\times10^{-11}$	$(1.3\pm0.4)\times10^{-11}$	$(0.5\pm0.2)\times10^{-11}$	$(5.5\pm0.8)\times10^{-12}$	$(8.8\pm0.3)\times10^{-12}$	$(5.5\pm0.8)\times10^{-12}$
τ_D [s]	$(1.2\pm0.3)\times10^{-4}$	$(0.7\pm0.2)\times10^{-4}$	$(1.5\pm0.5)\times10^{-4}$	$(1.0\pm0.1)\times10^{-4}$	$(0.7\pm0.2)\times10^{-4}$	$(1.0\pm0.1)\times10^{-4}$
A_D [s^{-2}]	$(1.2\pm0.4)\times10^{9}$	$(1.0\pm0.3)\times10^{9}$	$(2.1\pm0.9)\times10^{9}$	$(3.5\pm0.3)\times10^{9}$	$(1.3\pm0.2)\times10^{9}$	$(4.3\pm0.4)\times10^{9}$
τ_R [s]	$(2.1\pm0.5)\times10^{-8}$	$(1.1\pm0.3)\times10^{-8}$	$(4.4\pm0.9)\times10^{-8}$	$(1.6\pm0.3)\times10^{-8}$	$(1.1\pm0.3)\times10^{-8}$	$(3.7\pm0.5)\times10^{-8}$
A_R [s^{-2}]	$(0.7\pm0.2)\times10^{8}$	$(1.0\pm0.3)\times10^{8}$	$(0.8\pm0.1)\times10^{8}$	$(1.5\pm0.2)\times10^{-8}$	$(2.0\pm0.3)\times10^{8}$	$(0.9\pm0.1)\times10^{8}$
$A_{FM}J_{FM}$ [s^{-1}]	(6.1 ± 0.9)	(5.8 ± 0.6)		(7.1 ± 0.8)	(8.4 ± 0.2)	
Sum of the squared differences	211	63		942	661	

with the literature values from molecular dynamics.[53,56] There is little experimental evidence pinpointing the numbers of 'affected' lipids. However, in a recent commentary Evans[75] correlated the calculated energy (derived from micromechanical measurements of PC:cholesterol interaction at different compositions, with the area per lipid (from ^{2}H NMR analysis). It is interesting that the suggested optimal PC:cholesterol cluster cohesion energy occurs at a ratio of 5:2, which compares reasonably with our N^{aff} values.

Finally, examination of the physical parameters used in the optimal simulations shows that the diffusional and rotational processes become slower for affected lipids. The bending elastic modulus k increases by a factor of ~5.5 in the l_o phase, which is consistent with a more rigid and ordered structure. In fact the profiles are particularly sensitive to changes in κ. All these changes in the extracted parameters are consistent with the anticipated effect of cholesterol ordering on local dynamics. The amplitude pre-factors do not show very large changes between the populations. However, the variations were greater for the case of 25 mol% cholesterol (see Tables 3 and 4). Again, this can be attributed to the increased influence of the cholesterol dynamics. As expected therefore, the simulation, after optimising N^{aff} through the statistical analysis, provides slightly closer agreement with experiment for 10 mol% cholesterol.

3. Conclusions

We find that the ^{1}H relaxation profiles are more consistent with the partitioning of the lipid molecules into affected and unaffected portions, than with a single averaged phase. Taking into account the coarseness of the N^{aff} sampling, Figure 4 and 5, and the quality of the NMRD data (given the high ^{1}H dilution in the colloidal D_2O samples) we do not attribute any significance to the slight differences in N^{aff} obtained for the two compositions, Table 3 and 4. Hence for compositions up to 25 mol% cholesterol, we conclude that each sterol molecule orders three DOPC molecules, in agreement with a great many computational studies.[28,29,52,53,55,62–64]

It is apparent that the observation or non-observation of domains depends strongly on the sensitive timescale of the relevant technique. So for instance PFG-NMR provides an averaged view, given the rapid exchange timescale between the populations and the phase encoding times that are used. Similarly, ^{2}H NMR lineshape studies usually present spectral super-positions wherein the domains are in the slow exchange limit. FFC NMR relaxometry, while providing data which is sensitive to a broad range of motions, remains in the weak collision limit, $\tau_c \ll T_1$, at all ν_0 values for unilamellar vesicles. Hence the response is always in the slow motion limit and the data allows the two populations to be identified. Hence, using the FFC NMR approach it is not possible to directly obtain information on the rate of lipid exchange between the pools.

We have now validated the fast field-cycling approach for studying dynamics over a wide timescale for single component liposomes of different curvature and as a function of temperature[12,14] and for multi-component liposomes. The specific advantages are the ability to provide information on membrane rigidity and lipid lateral mobility from a single experiment on intact highly curved liposomal membranes of differing compositions. Hence the approach may add to the insights that can be gained from the array of physicochemical and computational techniques currently being used. In particular, the approach provides the elastic modulus of the membrane, and insights into local ordering in the vicinity of cholesterol. The latter is normally only obtainable from simulation.

In ongoing work we will exploit these advantages to evaluate the effect of temperature an isotonic strength of the medium on the key parameters derived for binary compositions of cholesterol with both unsaturated and saturated phosphatidylcholines. This may throw further light on the character of the different lipid populations. We will also to extend the approach to complex compositions of naturally sourced lipids, which provide a better model of biological membranes and their domain structure.

Experimental Section

Reagents: 1,2-Dioleoyl-*sn*-glycero-3-phosphocholine (DOPC) was purchased as a lyophilized powders (>99%) from Avanti Polar Lipids (Alabaster, AL) and stored at −20 °C. Deuterium oxide (D_2O, purity 99.9%) was obtained from Apollo Scientific Limited (UK) and cholesterol (>99%) was purchased from Aldrich Chemical Co. (Milwaukee, WI). All reagents were used without further purification.

Liposome Preparation: Large unilamellar vesicle (LUV) suspensions of DOPC of different vesicle sizes, 68 and 80 nm in radius, were prepared using established techniques. Uniform lipid/cholesterol mixtures were prepared by dissolving ~70 mg DOPC and 10 or 25 mol% cholesterol in 2 mL $CHCl_3$. The solvent was removed under a slow stream of N_2 over 24 h. Liposomes were prepared by hydrating the mixtures in 1.5 mL deuterium oxide (5 M proton, 0.06 M lipid) under a constant flow of Ar. The residual 0.1% HDO in the D_2O corresponds to a ^{1}H concentration of *c.* 0.05 M, which is a relatively low concentration for FFC NMR. The technique, like all low field NMR techniques, is highly insensitive which largely precludes the use of isotopic substitution with ^{2}H to provide site specific ^{1}H information. Hence the ratio of lipid to HDO ^{1}H is ~100:1 and we can be confident that the measured ^{1}H signal arises from the lipid ^{1}H component. The suspensions were heated above the main phase transition, T_m, to ~22 °C for 24 h, followed by three heating/cooling/shaking cycles to ensure a homogeneous preparation. Following hydration, the vesicle suspensions were exposed to six freeze–thaw cycles using liquid N_2 and warm water (40 °C), then passed at least eleven times through an Avanti Polar Lipids mini-extruder (Alabaster, AL) containing polycarbonate membranes with a pore size of 0.2 or 0.1 μm (Whatman Nuclepore; Clifton, NJ). The extrusion process was carried out above T_m in an AtmosBag glovebag (Aldrich Chemical Co.; Milwaukee, WI). It was found that as the% cholesterol was increased the extrusion process became more difficult, and more physical force was required. However, extrusion was successful in each case; the polycarbonate membrane survived the process intact, the widths of the DLS size distributions were comparable, and the samples were comparably stable.

Dynamic Light Scattering: The average sizes of the unilamellar liposome suspensions were determined using a High-Performance Particle Sizer HPPS (Malvern Instruments; Malvern, U.K.) using a detection angle of 173° and a 3 mW He-Ne laser operating at a wave-

length of 633 nm. The mean hydrodynamic diameter is determined from the rate of fluctuation of the intensity of scattered light.

Relaxation Rate Dispersion Experiments: ^{1}H relaxation rate dispersions (also termed NMRD profiles) were measured using the FFC NMR technique[11] with a Spinmaster FFC-2000 Fast Field-Cycling NMR Relaxometer (Stelar; Mede, Italy) for liposome samples of 1 mL volume. In all cases a polarization magnetic field of 0.329 T (equivalent to 14 MHz for ^{1}H) was used, which was switched on for a period of 0.5 s to generate sample magnetization. The value of the acquisition field was 0.217 T (9.25 MHz). A field slew rate of 0.47 T ms^{-1} (20 MHz ms^{-1}) was used in all cases, with a switching time of 1.5 ms to allow the magnetic field to settle. A digitization rate of 1 MHz was used for acquisition, while the dead time of the spectrometer was about 20 μs. The FID was sampled with 512 points in the time range 25–540 μs, after the front edge of the 90° pulse, which was of 7.5 μs duration. It should be noted that the FFC NMR approach uses fast switching, low-resolution (spatially inhomogeneous) electromagnets, and thus provides no spectroscopic resolution. The acquired signal contains unresolved contributions from all the ^{1}H nuclei within the sample; phospholipids and cholesterol, with the former predominant. It should be noted that any broadening due to the cholesterol that would be observable using high resolution NMR is masked by the B_0 inhomogeneity.
The relaxation rates, R_1, were determined from the magnetization recovery curves. The R_1 values were not sensitive to the time window over which the FID was sampled. The spin relaxation process for all samples was found to be mono-exponential, within error, at all frequencies. Sample temperature was controlled to within about 0.5 K using the Spinmaster Variable Temperature Controller. Temperatures were calibrated externally using a Cu–Al thermocouple in a 10 mm NMR tube. The time for each experiment was limited by the stability of the suspensions. 64 scans were used at each frequency and the total measurement time was 24 h. It was verified by NMR and DLS that the suspensions remained unchanged after the total time of the experiment. After several days, changes were observed in both R_1 and the hydrodynamic size. Profiles were measured within the frequency range from 30 kHz to 15.2 MHz in the liquid crystalline phase for liposomes of DOPC containing 10 mol% and 25 mol% of cholesterol. We find that at lower frequencies the local field becomes dominant and hence the magnetization does not evolve according to T_1, at higher frequencies the frequency dependence becomes essentially non-dispersive.[12] Experiments were performed on liposome suspensions with average hydrodynamic radii of 80 and 68 nm, at 298 K.

Simulation of the Relaxation Rate Dispersions: For this task we adopted the systematic approach already discussed by us previously[12, 14] with small modifications: 1) The relevant physical parameters were fixed within their most probable intervals, using literature values. 2) The frequency-independent contribution to the optimal parameter set was adjusted to within their most probable intervals. 3) Fine adjustments were made to the amplitudes (pre-factors) of each spectral density contribution, if required. The optimal simulation was obtained by manually minimizing the sum of the squared differences between the simulated curve and the experimental data.

Keywords: cholesterol effect · fast field-cycling NMR · lipid bilayers · molecular dynamics · NMR spectroscopy

[1] S. E. Veatch, S. L. Keller, *Biochim. Biophys. Acta* **2005**, *1746*, 172 – 185.
[2] A. Filippov, G. Orädd, G. Lindblom, *Biophys. J.* **2003**, *84*, 3079 – 3086.
[3] M. R. Vist, J. H. Davis, *Biochemistry* **1990**, *29*, 451 – 464.
[4] T. H. Huang, C. W. B. Lee, S. K. Dasgupta, A. Blume, R. G. Griffin, *Biochemistry* **1993**, *32*, 13277 – 13287.
[5] P. F. F. Almeida, W. L. C. Vaz, T. E. Thompson, *Biochemistry* **1992**, *31*, 6739 – 6747.
[6] F. S. Ariola, Z. Li, C. Cornejo, R. Bittman, A. A. Heikal, *Biophys. J.* **2009**, *96*, 2696 – 2708.
[7] M. Fraňová, J. Repáková, P. Čapková, J. M. Holopainen, I. Vattulainen, *J. Phys. Chem. B* **2010**, *114*, 2704 – 2711.
[8] A. Filippov, G. Orädd, G. Lindblom, *Biophys. J.* **2007**, *93*, 3182 – 3190.
[9] H. A. Scheidt, D. Huster, K. Gawrisch, *Biophys. J.* **2005**, *89*, 2504 – 2512.
[10] H. C. Gaede, K. Gawrisch, *Biophys. J.* **2003**, *85*, 1734 – 1740.
[11] R. Kimmich, E. Anoardo, *Progr. NMR Spectrosc.* **2004**, *44*, 257 – 320.
[12] C. J. Meledandri, J. Perlo, E. Farrher, D. F. Brougham, E. Anoardo, *J. Phys. Chem. B* **2009**, *113*, 15532 – 15540.
[13] E. Rommel, F. Noack, P. Meier, G. Kothe, *J. Phys. Chem.* **1988**, *92*, 2981 – 2987.
[14] J. Perlo, C. J. Meledandri, E. Anoardo, D. F. Brougham, *J. Phys. Chem. B* **2011**, *115*, 3444 – 3451.
[15] M. F. Roberts, A. G. Redfield, *J. Am. Chem. Soc.* **2004**, *126*, 13765 – 13777.
[16] M. F. Roberts, A. G. Redfield, U. Mohanty, *Biophys. J.* **2009**, *97*, 132 – 141.
[17] V. N. Sivanandam, J. Cai, A. G. Redfield, M. F. Roberts, *J. Am. Chem. Soc.* **2009**, *131*, 3420 – 3421.
[18] G. Lipari, A. Szabo, *J. Am. Chem. Soc.* **1982**, *104*, 4546 – 4559.
[19] A. Szabo, *Ann. N. Y. Acad. Sci.* **1986**, *482*, 44 – 50.
[20] J. Henriksen, A. C. Rowat, J. H. Ipsen, *Eur. Biophys. J.* **2004**, *33*, 732 – 741.
[21] *Handbook of Chemistry and Physics, 74th ed.* (Ed.: D. R. Lide), CRC Press, Boca Raton, FL **1993 – 1994**.
[22] M. Vilfan, G. Althoff, I. Vilfan, G. Kothe, *Phys. Rev. E* **2001**, *64*, 022902.
[23] M. Bloom, E. Evans, O. G. Mouritsen, *Q. Rev. Biophys.* **1991**, *24*, 293 – 397.
[24] G. Althoff, D. Frezzato, M. Vilfan, O. Stauch, O. Schubert, I. Vilfan, G. J. Moro, G. Kothe, *J. Phys. Chem. B* **2002**, *106*, 5506 – 5516.
[25] G. Althoff, O. Stauch, M. Vilfan, D. Frezzato, G. J. Moro, P. Hausser, R. Schubert, G. Kothe, *J. Phys. Chem. B* **2002**, *106*, 5517 – 5526.
[26] P. G. Saffman, M. Delbruch, *Proc. Natl. Acad. Sci. USA* **1975**, *72*, 3111 – 3113.
[27] Y. Umegawa, N. Matsumori, T. Oishiv, M. Murata, *Biochemistry* **2008**, *47*, 13463 – 13469.
[28] O. Edholm, A. M. Nyberg, *Biophys. J.* **1992**, *63*, 1081 – 1089.
[29] A. J. Robinson, W. G. Richards, P. J. Thomas, M. M. Hann, *Biophys. J.* **1995**, *68*, 164 – 170.
[30] J. H. Ipsen, O. G. Mouritsen, M. Bloom, *Biophys. J.* **1990**, *57*, 405 – 412.
[31] W. Hung, M. Lee, F. Chen, H. W. Huang, *Biophys. J.* **2007**, *92*, 3960 – 3967.
[32] S. Tristram-Nagle, H. I. Petrache, J. F. Nagle, *Biophys. J.* **1998**, *75*, 917 – 925.
[33] J. C. Mathai, S. Tristram-Nagle, J. F. Nagle, M. L. Zeidel, *J. Gen. Physiol.* **2008**, *131*, 69 – 76.
[34] J. Pan, S. Tristram-Nagle, N. Kučerka, J. F. Nagle, *Biophys. J.* **2008**, *94*, 117 – 124.
[35] H. P. Duwe, E. Sackmann, *Phys. A* **1990**, *163*, 410 – 428.
[36] Y. Liu, J. F. Nagle, *Phys. Rev. E* **2004**, *69*, 040901.
[37] J. Pan, T. T. Mills, S. Tristram-Nagle, J. F. Nagle, *Phys. Rev. Lett.* **2008**, *100*, 198103.
[38] T. P. Trouard, A. A. Nevzorov, T. M Alam, C. Job, J. Zajicek, M. F. Brown, *J. Chem. Phys.* **1999**, *110*, 8802 – 8818.
[39] K. Weisz, G. Gröbner, C. Mayer, J. Stohrer, G. Kothe, *Biochemistry* **1992**, *31*, 1100 – 1112.
[40] R. Kimmich, G. Schnur, A. Scheuermann, *Chem. Phys. Lipids* **1983**, *32*, 271 – 322.
[41] V. K. Mishra, G. M. Anantharamaiah, J. P. Segrest, M. N. Palgunachari, M. Chaddha, S. W. S. Sham, N. R. Krishna, *J. Biol. Chem.* **2006**, *281*, 6511 – 6519.
[42] K. Tamm, H. M. McConnell, *Biophys. J.* **1985**, *47*, 105 – 113.
[43] M. Przybylo, J. Sykora, J. Humpolickova, A. Benda, A. Zan, M. Hof, *Langmuir* **2006**, *22*, 9096 – 9099.
[44] N. Kahya, D. Scherfeld, K. Bacia, P. Schwille, *J. Struct. Biol.* **2004**, *147*, 77 – 89.
[45] D. Scherfeld, N. Kahya, P. Scwille, *Biophys. J.* **2003**, *85*, 3758 – 3768.
[46] N. Kahya, D. Scherfeld, K. Bacia, B. Poolman, P. Schwille, *J. Biol. Chem.* **2003**, *278*, 28109 – 28115.
[47] A. Filippov, G. Orädd, G. Lindblom, *Langmuir* **2003**, *19*, 6397 – 6400.

[48] K. Simons, W. L. C. Vaz, *Ann. Rev. Biophys. Biomol. Struct.* **2004**, *33*, 269 – 295.
[49] E. S. Wu, K. Jacobson, D. Papahadjopoulos, *Biochemistry* **1977**, *16*, 3936 – 3941.
[50] E. Lindahl, *O. Edholm, J. Chem. Phys.* **2001**, *115*, 4938 – 4950.
[51] N. O. Petersen, S. I. Chan, *Biochemistry* **1977**, *16*, 2657 – 2667.
[52] S. W. Chiu, E. Jakobsson, R. J. Mashl, H. L. Scott, *Biophys. J.* **2002**, *83*, 1842 – 1853.
[53] P. Jedlovszky, M. Mezei, *J. Phys. Chem. B* **2003**, *107*, 5311 – 5321.
[54] S. A. Pandit, S. W. Chiu, E. Jakobsson, A. Grama, H. L. Scott, *Langmuir* **2008**, *24*, 6858.
[55] J. Dai, M. Alwarawrah, J. Huang, *J. Phys. Chem. B* **2010**, *114*, 840 – 848.
[56] D. M. Engelman, J. M. Rothman, *J. Biol. Chem.* **1972**, *247*, 3694 – 3697.
[57] M. J. L. de Lange, M. Bonn, M. Muller, *Chem. Phys. Lipids* **2007**, *146*, 76 – 84.
[58] M. A. Davies, H. F. Schuster, J. W. Brauner, R. Mendelsohn, *Biochemistry* **1990**, *29*, 4368 – 4373.
[59] D. E. Warschawski, P. F. Devaux, *Eur. Biophys. J.* **2005**, *34*, 987 – 996.
[60] J. A. Clarke, J. M. Seddon, R. V. Law, *Soft Matter* **2009**, *5*, 369 – 378.
[61] a) A. Kusumi, W. K. Subczynski, M. Pasenkiewicz-Gierula, J. S. Hyde, H. Merke, *Biochim. Biophys. Acta* **1986**, *854*, 307 – 317; b) A. Kusumi, M. Pasenkiewicz-Gierula, *Biochemistry* **1988**, *27*, 4407 – 4415; c) M. Pasenkiewicz-Gierula, W. K. Subczynski, A. Kusumi, *Biochemistry* **1990**, *29*, 4059 – 4069.
[62] K. Tu, M. L. Klein, D. J. Tobias, *Biophys. J.* **1998**, *75*, 2147 – 2156.
[63] A. M. Smondyrev, M. L. Berkowitz, *Biophys. J.* **1999**, *77*, 2075 – 2089.
[64] S. Y. Bhide, Z. Zhang, M. L. Berkowitz, *Biophys. J.* **2007**, *92*, 1284 – 1295.
[65] L. Miao, M. Nielsen, J. Thewalt, J. H. Ipsen, M. Bloom, M. J. Zuckermann, O. G. Mouritsen, *Biophys. J.* **2002**, *82*, 1429 – 1444.
[66] G. Lindblom, L. Johansson, G. Arvidson, *Biochemistry* **1981**, *20*, 2204 – 2207.
[67] M. Bloom, O. G. Mouritsen, *Can. J. Chem.* **1988**, *66*, 706 – 712.
[68] Y. K. Shin, J. H. Freed, *Biophys. J.* **1989**, *55*, 537 – 550.
[69] H. L. Scott, *Biophys. J.* **1991**, *59*, 445 – 455.
[70] H. Ohvo-Rekilä, B. Ramstedt, P. Leppimäki, J. P. Slotte, *Prog. Lipid Res.* **2002**, *41*, 66 – 97.
[71] C. Hofsäß, E. Lindahl, O. Edholm, *Biophys. J.* **2003**, *84*, 2192 – 2206.
[72] H. Martinez-Seara, T. Róg, M. Pasenkiewicz-Gierula, I. Vattulainen, M. Karttunen, R. Reigada, *Biophys. J.* **2008**, *95*, 3295 – 3305.
[73] F. de Meyer, B. Smit, *Proc. Natl. Acad. Sci. USA* **2009**, *106*, 3654 – 3658.
[74] M. Alwarawrah, J. Dai, J. Huang, *J. Phys. Chem. B* **2010**, *114*, 7516 – 7523.
[75] E. Evans, W. Rawicz, B. A. Smith, *Faraday Discuss.* **2013**, *161*, 591.

Received: November 12, 2013
Published online on January 31, 2014